Supporting Information

The $Sb@Ni_{12}@Sb_{20}^{1-/1+}$ and $Sb@Pd_{12}@Sb_{20}^{n}$ Cluster Anions Where n = +1, -1, -3, -4: Multi-Oxidation State Clusters of Interpenetrating Platonic Solids

Yi Wang,[†] Melanie Moses-DeBusk,[†] Lauren Stevens,[†] Junkai Hu,[†] Peter Zavalij,[†] Kit Bowen,[‡] Brett I. Dunlap,[#] Bryan Eichhorn[†,*]

[†] Department of Chemistry and Biochemistry, University of Maryland, College Park, MD 20742

[‡] Departments of Chemistry and Materials Science, Johns Hopkins University, Baltimore, MD 21218

[#] US Naval Research Laboratory, Code 6189, Washington, D.C. 20746-5342

E-Mail: eichhorn@umd.edu

Experimental Section

General Data. All reactions were carried out in a nitrogen atmosphere dry box (Vacuum Atmosphere Co). The Laser Desorption/Ionization time-of-flight (LDI–TOF, Shimadzu Axima-CFR) mass spectra were recorded in the negative ion mode with a nitrogen pulsed laser with wavelength 337nm, 10Hz, the pulse power 140 μJ. EDX analyses were performed on Hitachi SU-70 SEM, operated at an acceleration voltage of 10 keV. The analysis showed the presence of P, Pd, and Sb, and the absence of other elements heavier than P.

LDI-TOF MS data were collected by loading the crystals of $[Bu_4P]_3[Sb@Pd_{12}@Sb_{20}]$•3.5en and $[Bu_4P]_4[Sb@Pd_{12}@Sb_{20}]$•4tol on carbon tape on the LDI -MS sample holder or by directly depositing the corresponding reaction mixtures on the LDI-MS sample holder. Direct desorption from the crystalline samples at high laser pulse energies generated intense ion beams that resulted in mass shifts of the ions (lower m/z in negative ion mode and higher m/z in positive ion mode) due to distorted electric fields. Lowering the laser pulse energies decreased the signal intensity but also removed the mass shift (Figure S2). The shifts were corrected in the reported spectra. The mass envelopes were fit by using the Gauss Model in OriginPro 9. The peak position and full width at

half maximum (FWHM) values were fixed before the simulation and were calculated by Mmass Software Version 3.

Chemicals. Melts of nominal composition of K_3Sb_7 and K_5Sb_4 were prepared by fusion of stoichiometric ratios of the elements at high temperature (~1100 °C). The elements were loaded into quartz tubes in a nitrogen atmosphere dry box and then sealed under vacuum. CAUTION: the fusion process can be very exothermic and the reactions should be conducted behind blast shields on small scales (< 5 g) using full protective gear. $Pd(PPh_3)_4$, Bu_4PBr and ethylenediamine (en) were all purchased from Sigma-Aldrich. $Ni(COD)_2$ was purchased from STREM Chemicals (COD = cyclooctadiene). Anhydrous ethylenediamine(en) vacuum distilled from K_4Sn_9 and stored under N_2. Toluene was distilled from sodium under N_2 and stored under N_2.

Preparation of $[Bu_4P]_3[Sb@Pd_{12}@Sb_{20}]$•3.5en. In vial 1, K_3Sb_7 (62.7mg, 0.064mmol), Bu_4PBr (76.8mg, 0.22mmol) were dissolved in en (~ 2mL) and stirred for 1h, yielding a dark red solution. In vial 2, $Pd(PPh_3)_4$ (24.2 mg, 0.021mmol) was dissolved in toluene (~4 mL), yielding a yellow solution. The solution from vial 2 was added dropwise to vial 1 and the mixture was stirred for 16 h, yielding a dark reddish-brown solution. The solution was then filtered through tightly packed glass wool. The filtered solution was heated at 60 ºC for 3h and filtered again. Solution was stored in the dry-box for crystallization. After about a week, small black needle crystals of $[Bu_4P]_3[Sb@Pd_{12}Sb_{20}]$•3.5en. precipitated in low yield (15% based on $Pd(PPh_3)_4$). Small amounts (ca. 2%) of the $[Bu_4P]_4[Sb@Pd_{12}Sb_{20}]$•4tol crystals also form in this reaction.

Preparation of $[Bu_4P]_4[Sb@Pd_{12}@Sb_{20}]$•4tol In vial 1, K_5Sb_4 (34.6mg, 0.051mmol), Bu_4PBr (69.6mg, 0.21mmol) were dissolved in en (~ 2mL) and stirred for 1h, yielding a dark red solution. In vial 2, $Pd(PPh_3)_4$ (23.6 mg, 0.20mmol) was dissolved in toluene (~4 mL), yielding a yellow solution. The solution from vial 2 was added dropwise to vial 1 and the mixture was stirred for 16 h, yielding a dark reddish solution. The solution was then filtered through tightly packed glass wool. The filtered solution was heated at 60 ºC for 3h and filtered again. Solution was stored in the dry-box for crystallization. After about a week, small dark-brown plate-like crystals of $[Bu_4P]_4[Sb@Pd_{12}@Sb_{20}]$•4tol precipitated in low yield (~5% based on $Pd(PPh_3)_4$) .

Preparation of $[Sb@Ni_{12}Sb_{20}]^{n-}$(n=3/4) In vial 1, K_3Sb_7 (75.6mg, 0.078mmol), Bu_4PBr (81.6mg, 0.24mmol) were dissolved in en (~ 1.5mL) and stirred for 1h, yielding a dark red solution. In vial 2, $Ni(COD)_2$ (43.0 mg, 0.156mmol) was dissolved in toluene (~1ml), yielding a yellow/orange

solution. The solution from vial 2 was added dropwise to vial 1 and the mixture was stirred for 4h, yielding a black-brown solution. The solution was then filtered through tightly packed glass wool. The filtered solution was heated at 60 ºC for 1h and filtered again. The mass spectra of the reaction mixture confirmed the existence of the anion $Ni_{12}Sb_{21}^{1-}$ although no $Ni_{12}Sb_{21}^{n-}$ (n=3/4)-containing crystals were obtained.

Crystallographic Studies. $[Bu_4P]_3[Sb@Pd_{12}@Sb_{20}]$•3.5en. A suitable single crystal of $C_{55}H_{136}N_7OP_3Pd_{12}Sb_{21}$ (UM2880) was selected and measured on a Bruker Smart Apex2 CCD diffractometer.[1] The crystal was kept at 120(2) K during data collection. The integral intensity data were corrected for absorption using the multi-scan method of SADABS software.[2] The resulting minimum and maximum transmissions are 0.484 and 0.675, respectively. The structure was solved with the ShelXT program and refined with the XL program and Least Squares minimization using ShelX software package.[3] Number of restraints used = 1754. H atoms were positioned from geometric considerations and refined as riding on the attached atom with U_{iso} constrained to be 20% larger (50% for methyl groups) than U_{eqv} of the attached atom. The orientations of methyl groups in non-disordered moieties were optimized. The structure contains strongly disordered ethylenediamine solvent which was accounted for using the SQUEEZE procedure from Platon software (Spek, 1990).[4] The total amount of removed electron density corresponds to about 3.5 molecules of ethylenediamine per $Pd_{12}Sb_{21}$ cluster and was added to total composition in order to obtain accurate density, absorption coefficient and F000. One of three tetra-butyl phosphonium ions is disordered in two alternative positions. Therefore, the butyl tails were refined with geometry restrained to be similar and atomic displacement parameters to correspond to rigid body motions.

$[Bu_4P]_4[Sb@Pd_{12}@Sb_{20}]$•4tol. A suitable single crystal of $C_{92}H_{176}P_4Pd_{12}Sb_{21}$ (UM2887) was selected and measured on a Bruker Smart Apex II CCD diffractometer.[1] The crystal was kept at 150(2) K during data collection. The integral intensities were corrected for absorption using the multi-scan method in SADABS software.[2] The resulting minimum and maximum transmissions are 0.516 and 0.871, respectively. The structure was solved with the ShelXT program and refined with the XL program and Least Squares minimization using ShelX software package,[3] The number of restraints used = 98. H atoms were positioned from geometric considerations and refined as riding on the attached atom with U_{iso} constrained to be 20% larger (50% for methyl groups) than U_{eqv} of the

attached atom. The structure contains significantly disordered toluene solvates, which were accounted for using SQUEEZE procedure from Platon software (Spek, 1990).[4] Total amount of electron density "squeezed" out corresponded to approximately 8 toluene molecules per unit cell that was added to total composition in order to obtain correct density, absorption coefficient and F000. 2 of 4 butyl groups disordered in 2 alternative orientations and were refined with geometry and atomic displacement parameters restrained to be the same and corresponded to rigid body motions.

DFT Calculations. All-electron calculations using the DGauss DZVP double zeta orbital basis with matching A2 auxiliary basis set [5] using the analytic density-functional method [6] with exchange-correlation parameter 0.7 were used to compute electronic structures. A JMOL orbital contour of one of the degenerate HOMO states is given in Figure S6.

References:

1. Bruker (**2010**). Apex2. Bruker AXS Inc., Madison, Wisconsin, USA.
2. Sheldrick, G. M. Acta Cryst. 2008, A64, 112-122.
3. Sheldrick, G. M.(**2014**) SHELXL-2014.University of Gottingen, Germany
4. Spek A. L. *Acta Cryst.* **2015**, C71, 9–18
5. N. Godbout, D. R. Salahub, J. Andzelm, E. Wimmer, *Can. J. Chem*. **1992, 70***,* 560.
6. B. I. Dunlap, *J. Phys. Chem*. **2003**, A107, 10082.

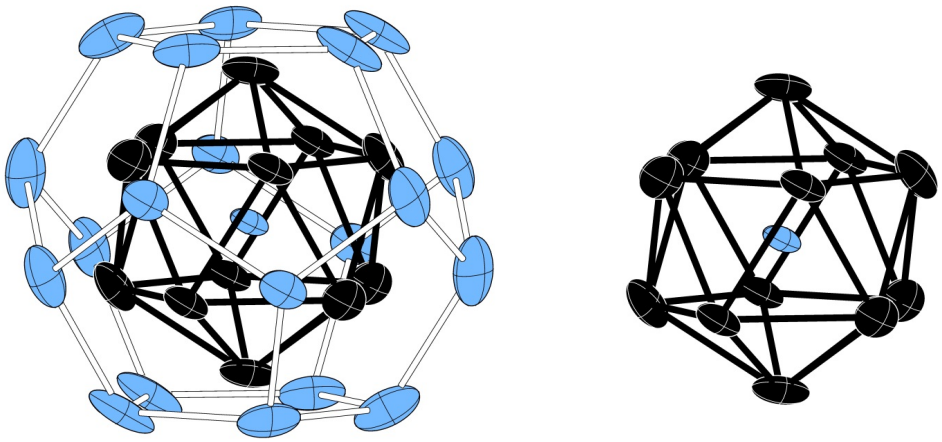

(A) **(B)**

Figure S1 ORTEP drawings of (A) the $[Sb@Pd_{12}@Sb_{20}]^{3-}$ ion and (B) the $[Pd_{12}(\mu_{12}\text{-}Sb)]^{3-}$ subunit. Sb is blue, Pd is black, thermal ellipsoids are set at 50% probability level. The bonds between the $[Pd_{12}(\mu_{12}\text{-}Sb)]^{3-}$ and Sb_{20} subunits have been omitted for clarity.

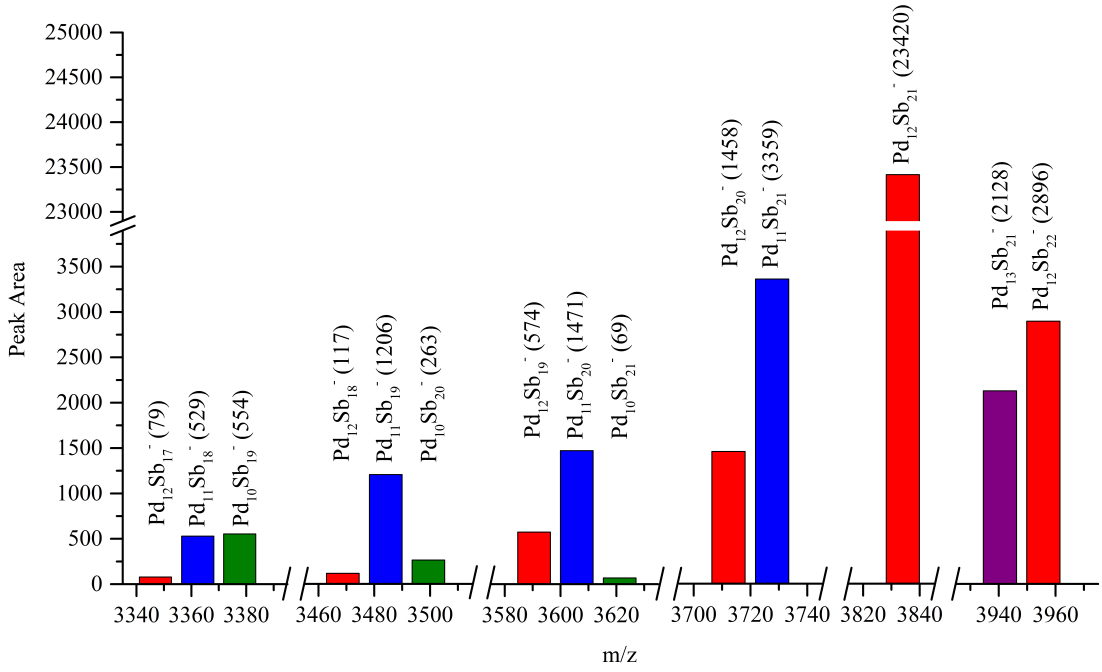

Figure S2. Distribution of the parent ion $Pd_{12}Sb_{21}^-$ and its derivative anions.(e.g. $Pd_{12}Sb_{21-x}^{1-}$ (x = 1-10) and $Pd_{12-y}Sb_{21-x}^{1-}$ (y = 1-3))

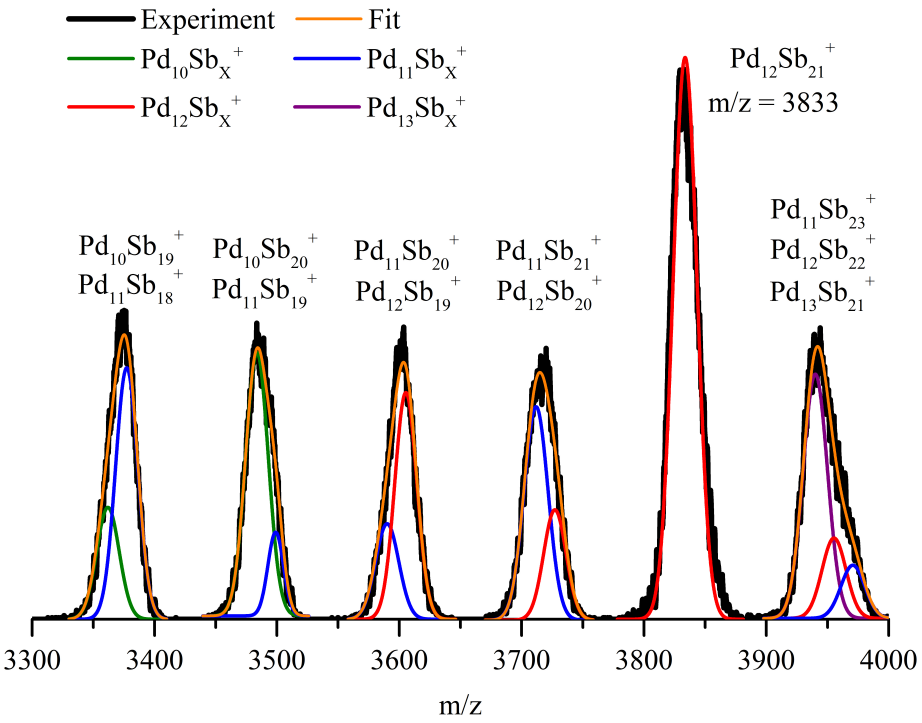

Figure S3. Positive-ion mode LDI–TOF mass spectra of $[Bu_4P]_3[Sb@Pd_{12}Sb_{20}]$•3.5en salt deposited on carbon tape shows a strong parent ion peak $Pd_{12}Sb_{21}^+$ ion in the gas phase, along with other $Pd_{12-y}Sb_{21-x}^+$ clusters.

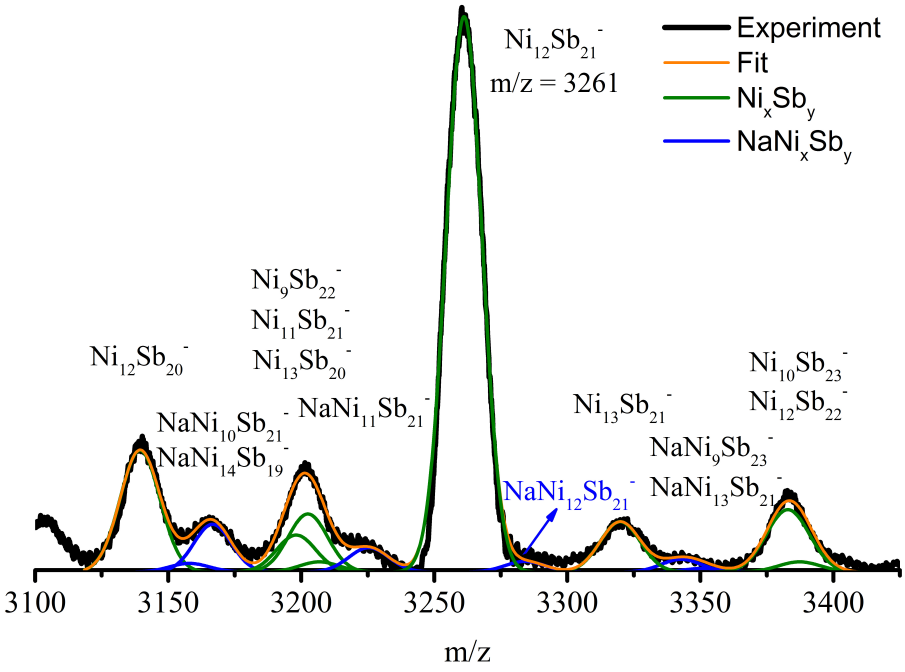

Figure S4. Negtive-ion mode LDI–TOF mass spectra of black precipitates of $Sb@Ni_{12}@Sb_{20}^{n-}$ salts. Blue arrow denote the sodium-coordinated parent ion pairs $NaNi_{12}Sb_{21}^-$.

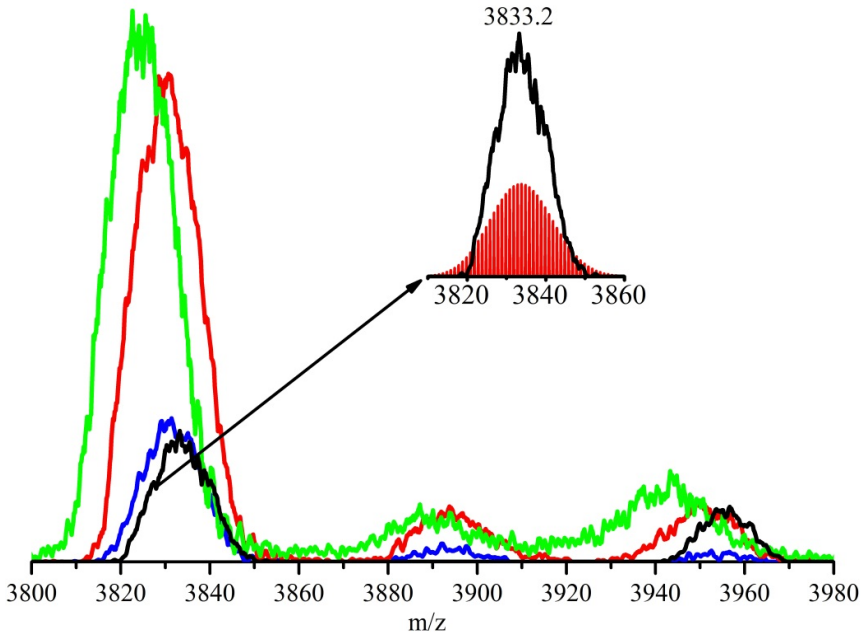

Figure S5. Negative-ion mode LDI–TOF mass spectra of the same $Pd_{12}Sb_{21}^-$ sample with different pulse energy (green curve: 160μJ, red curve: 140 μJ, blue curve: 135 μJ and black curve:112 μJ). (Inset) Enlarged view of the $Pd_{12}Sb_{21}^-$ mass envelope along with its simulated pattern.

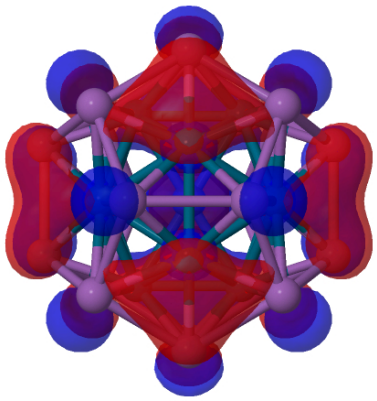

Figure S6. JMOL plot of the 36 t_{1u} molecular orbital (HOMO) of $Sb@Pd_{12}@Sb_{20}^{3-}$ showing the radial Sb-Pd overlap.

Table S1. Summary of structural data[a] for $[E@M_{12}@E_{20}]^{n-}$ Clusters (E=As, M=Ni, n=3[b]; E=Sb, M=Pd, n=3 and 4; E= Sn, M=Cu, n=12, cation=Na, K[c]).

	Bonding Length	P-M_{12}	M-M (M_{12})	P-P (P_{20})	M-P (M_{12}-P_{20})
$[As@Ni_{12}@As_{20}]^{3-}$	Minimum/Å	2.5414(6)	2.6674(8)	2.7109(6)	2.3805(7)
	Maximum/Å	2.5801(6)	2.7091(7)	2.7932(7)	2.4203(7)
	Average/Å	2.557 (2)	2.689(4)	2.752(3)	2.395(5)
$[Sb@Pd_{12}@Sb_{20}]^{3-}$	Minimum/Å	2.8243(19)	2.980(2)	3.080(2)	2.688(2)
	Maximum/Å	2.8818(19)	3.024(2)	3.139(2)	2.7496(19)
	Average/Å	2.856(20)	3.003(10)	3.109(34)	2.713(45)
Theory		2.8471	2.9936	3.1488	2.7585
$[Sb@Pd_{12}@Sb_{20}]^{4-}$	Minimum/Å	2.8342(12)	2.9895(14)	3.0850(3)	2.6998(13)
	Maximum/Å	2.8700(9)	3.0133(15)	3.1217(15)	2.7311(12)
	Average/Å	2.8538(3)	3.0009(5)	3.1063(5)	2.7114(6)
Theory	Minimum/Å	2.8346	2.9868	3.0781	2.7490
	Maximum/Å	2.8677	3.0111	3.1924	2.7925
	Average/Å	2.8512	2.9980	3.1566	2.7659
$[Sn@Cu_{12}@Sn_{20}]^{12-}$ (Na)	Minimum/Å	2.631(1)	2,742(2)	3.083(1)	2.718(2)
	Maximum/Å	2.631(2)	2.792(3)	3.133(1)	2.797(1)
	Average/Å	2.631(5)	2.766(12)	3.104(5)	2.766(9)
$[Sn@Cu_{12}@Sn_{20}]^{12-}$ (K)	Minimum/Å	2.622(1)	2.738(2)	3.076(1)	2.730(1)
	Maximum/Å	2.628(1)	2.780(2)	3.133(1)	2.781(1)
	Average/Å	2.625(3)	2.759(8)	3.097(5)	2.760(7)

[a] The M-E_{12} bond are to the central μ_{12} atom. The M-E bonds are to the outer E_{20} shell.

[b] Moses, M.; Fettinger, J.; Eichhorn, B. *Science* ***2003***, 300, 778-781.

[c] Stegmaier, S; Fässler, T. F. *J. Am. Chem. Soc.*, ***2011***, 133, 19758–19768.

Table S2 Ratio of the bond lengths in $[E@M_{12}@E_{20}]^{n-}$ Ions[a] (E=As, M=Ni, n=3[b];E=Sb, M=Pd, n=3 and 4; E= Sn, M=Cu, n=12, cation=Na, K[c]).

	M-E/ E-E	M-M/E-E	E-M_{12}/E-E	M-M/M-E	E-M_{12}/M-E	E-M_{12}/M-M
$[As@Ni_{12}@As_{20}]^{3-}$	0.8703	0.9771	0.9291	1.123	1.068	0.9509
$[Sb@Pd_{12}@Sb_{20}]^{3-}$	0.8726	0.9659	0.9186	1.107	1.053	0.9510
$[Sb@Pd_{12}@Sb_{20}]^{4-}$	0.8729	0.9661	0.9187	1.107	1.053	0.9510
$[Sn@Cu_{12}@Sn_{20}]^{12-}$ (Na)	0.8911	0.8911	0.8476	1.000	0.9512	0.9512
$[Sn@Cu_{12}@Sn_{20}]^{12-}$ (K)	0.8912	0.8909	0.8476	0.9996	0.9511	0.9514

[a] The M-E_{12} bond are to the central μ_{12} atom. The M-E bonds are to the outer E_{20} shell.

[b] Moses, M.; Fettinger, J.; Eichhorn, B. *Science **2003***, 300, 778-781.

[c] Stegmaier, S; Fässler, T. F. *J. Am. Chem. Soc.*, ***2011***, 133, 19758–19768

Table S3 Average Calculated Bond Lengths [Å] for the icosahedral fragment $[E@M_{12}]$ which reside at the center of an E_{20} dodecahedral cage (E=As, M=Ni; E=Sb, M=Pd; E= Sn, M=Cu)

			E-M distances			M-M distances			
Metal(M)	covalent radii of M[a] (Å)	diagonal distance (av) (Å)	average (Å)	range (Å)	variance $\sigma^2\times10^{-3}$	average (Å)	range (Å)	variance $\sigma^2\times10^{-3}$	d(E-M)/d(M-M)
Ni	1.24	5.115	2.557 (2)	0.0387	0.142	2.689 (4)	0.0398	0.115	0.9509
Pd (3-)	1.39	5.713	2.856(20)	0.0575	0.242	3.003(10)	0.044	0.143	0.9510
Pd (4-)	1.39	5.708	2.8538(3)	0.0358	0.176	3.0009(5)	0.0238	0.152	0.9510
Cu(Na)	1.32	5.741	2.631(5)	0	0	2.766(12)	0.050	0.264	0.9512
Cu(K)	1.32	5.736	2.625(3)	0.006	0.00981	2.759(8)	0.042	0.184	0.9514

[a]Data from ref * [b]Variance is defined as: $\sigma^2=[\sum_{i=1}^{N}(x_i-\bar{x})^2]/(N-1)$

* Cordero, B.; Gómez,V.; Platero-Prats, A. E.; Revés,M.; Echeverría, J.; Cremades,E.; Barragán, F.; Alvarez, S.; *Dalton Trans.*, **2008**, 2832–2838.

Table S4 Selected Crystallographic, Data Collection, and Refinement Data for $[Bu_4P]_3[Sb@Pd_{12}@Sb_{20}]$•3.5en and $[Bu_4P]_4[Sb@Pd_{12}@Sb_{20}]$•4tol.

	$[Bu_4P]_3[Sb@Pd_{12}@Sb_{20}]$•3.5en[a]	$[Bu_4P]_4[Sb@Pd_{12}@Sb_{20}]$ •4tol[a]
Empirical formula	C55H136N7OP3Pd12Sb21	C92H176P4Pd12Sb21
Formula weight	4822.16	5239.75
Temperature/K	120(2)	150(2)
Crystal system	monoclinic	monoclinic
Space group	P21/n	C2/m
a/Å	16.834(2)	19.3446(17)
b/Å	31.679(4)	20.8536(18)
c/Å	19.255(2)	19.6141(18)
α/°	90	90
β/°	106.8075(15)	117.1165(14)
γ/°	90	90
Volume/Å^3	9830(2)	7042.7(11)
Z	4	2
ρ_{cal} cg/cm^3	3.258	2.471
μ/mm-1	7.871	5.513
F(000)	8732.0	4822.0
Crystal size/mm^3	0.16 × 0.12 × 0.05	0.32 × 0.23 × 0.025
Radiation	Mo*Kα* (λ = 0.71073)	Mo*Kα* (λ = 0.71073)
2θ range for data collection/°	3.39 to 49.998	3.134 to 50
Index ranges	-20 ≤ h ≤ 20, -37 ≤ k ≤ 37, -22 ≤ l ≤ 22	-22 ≤ h ≤ 22, -24 ≤ k ≤ 24, -23 ≤ l ≤ 23
Reflections collected	98038	37812
Independent reflections	17274 [R_{int} = 0.0656, R_{sig} = 0.0580]	6380 [R_{int} = 0.0426, R_{sig} = 0.0343]
Data/restraints/parameters	17274/1754/948	6380/98/258
Goodness-of-fit on F^2	1.149	1.067
R_1/wR_2 [I>=2σ (I)]	0.0627, 0.1383	0.0594, 0.1278
R_1/wR_2 [all data]	0.1078, 0.1560	0.0750, 0.1328

[a]See the Crystallographic Studies Section for details on the refinement .